Imbalance entanglement: Symmetry decomposition of negativity

Eyal Cornfeld, Moshe Goldstein, and Eran Sela
Raymond and Beverly Sackler School of Physics and Astronomy, Tel-Aviv University, 6997801 Tel Aviv, Israel

(Received 8 April 2018; published 4 September 2018)

In the presence of symmetry, entanglement measures of quantum many-body states can be decomposed into contributions from distinct symmetry sectors. Here we investigate the decomposability of negativity, a measure of entanglement between two parts of a generally open system in a mixed state. While the entanglement entropy of a subsystem within a closed system can be resolved according to its total preserved charge, we find that negativity of two subsystems may be decomposed into contributions associated with their charge imbalance. We show that this charge-imbalance decomposition of the negativity may be measured by employing existing techniques based on creation and manipulation of many-body twin or triple states in cold atomic setups. Next, using a geometrical construction in terms of an Aharonov-Bohm-like flux inserted in a Riemann geometry, we compute this decomposed negativity in critical one-dimensional systems described by conformal field theory. We show that it shares the same distribution as the charge-imbalance between the two subsystems. We numerically confirm our field theory results via exact calculations for noninteracting particles based on a double-Gaussian representation of the partially transposed density matrix.

DOI: 10.1103/PhysRevA.98.032302

I. INTRODUCTION AND RESULTS

Negativity provides a measure of quantum entanglement between two subsystems A_1 and A_2 in a generally mixed state [1–10]. This state can be achieved when the full system $(A_1 \cup A_2) \cup B$ is in a pure state, after tracing out B, treated as the environment. In this case the usual von Neumann entropy of either A_1 or A_2 is not a measure of quantum entanglement and instead other measures have to be defined such as the negativity. The latter involves the nonstandard operation of a *partial transposition* on the density matrix $\rho_A \mapsto \rho_A^{\mathrm{T}_2}$. A density matrix ρ_A is unentangled if $\rho_A = \sum_i w^{(i)} \rho_{A_1}^{(i)} \otimes \rho_{A_2}^{(i)}$, where $\sum_i w^{(i)} = 1$ and ρ_{A_1} and ρ_{A_2} are positive-semidefinite density matrices of the two subsystems; after performing a partial transposition with respect to the subsystem A_2 on an unentangled density matrix $\rho_A^{\mathrm{T}_2} = \sum_i w^{(i)} \rho_{A_1}^{(i)} \otimes (\rho_{A_2}^{(i)})^{\mathrm{T}}$, it remains positive. One thus concludes that the presence of any negative eigenvalue in the spectrum $\{\lambda\}$ of $\rho_A^{\mathrm{T}_2}$, referred to as the negativity spectrum, must indicate entanglement between the two subsystems [1]. One hence defines the entanglement negativity as

$$\mathcal{N} \equiv \frac{1}{2}\left(\mathrm{Tr}\left|\rho_A^{\mathrm{T}_2}\right| - 1\right) = \sum_{\lambda<0} |\lambda| \tag{1}$$

such that nonvanishing negativity implies entanglement. Related entanglement measures are the Rényi negativities

$$R_n \equiv \mathrm{Tr}\left\{\left(\rho_A^{\mathrm{T}_2}\right)^n\right\} = \sum_\lambda \lambda^n, \quad \mathcal{N} = \lim_{n\to 1/2} \frac{1}{2}(R_{2n} - 1). \tag{2}$$

Knowledge of Rényi negativities may be used, via various techniques, to find either the entanglement negativity [11] or the entire negativity spectrum [4].

Over recent years there has been growing interest in the negativity of many-body systems. Key progress was achieved using field theory methods specifically focusing on critical systems [4,12–16], supplemented by numerical techniques [4,17]. Interesting aspects of negativity were also discussed in symmetric many-qubit Dicke states [18–20], in topological gapped phases [21–23], and in disordered systems [24,25]. Owing to the nonstandard operation of partial transposition, obtaining the negativity spectrum is challenging even for free-fermion systems [16,26].

In this paper we study a general symmetry decomposition of the negativity. Recently, it has been shown that entanglement entropy admits a charge decomposition which can be both computed and measured [27–29]. This is based on a block-diagonal form of the density matrix in the presence of symmetries and allows one to identify contributions of entanglement entropy from individual charge sectors. It is natural to ask whether negativity admits a similar symmetry decomposition. This is nontrivial due to the involved operation of partial transposition on the density matrix.

We find that instead of a decomposition according to the total charge, negativity admits a resolution by the charge imbalance in the two subsystems. This holds whenever there is a conserved extensive quantity $\hat{O}$ in the joint Hilbert space of the system $A = A_1 \cup A_2$ and the environment B, i.e., $\hat{O}_{(A_1\cup A_2)\cup B} = \hat{O}_1 + \hat{O}_2 + \hat{O}_B$. We show that the negativity spectrum is then partitioned, $\{\lambda_i\} = \bigcup_Q \{\lambda_{i_Q}\}$, by the eigenvalues of an imbalance operator $\hat{Q} \sim \hat{O}_1 - \hat{O}_2$; see Eq. (8) for the precise definition. Examples for such extensive quantities may be the particle number $\hat{N}_{(A_1\cup A_2)\cup B} = \hat{N}_1 + \hat{N}_2 + \hat{N}_B$ or magnetization $\hat{S}^z_{(A_1\cup A_2)\cup B} = \hat{S}^z_1 + \hat{S}^z_2 + \hat{S}^z_B$.

This finding is particularly appealing in view of its experimental feasibility. Based on a proposal [30,31] which had been experimentally implemented [32] to measure the Rényi

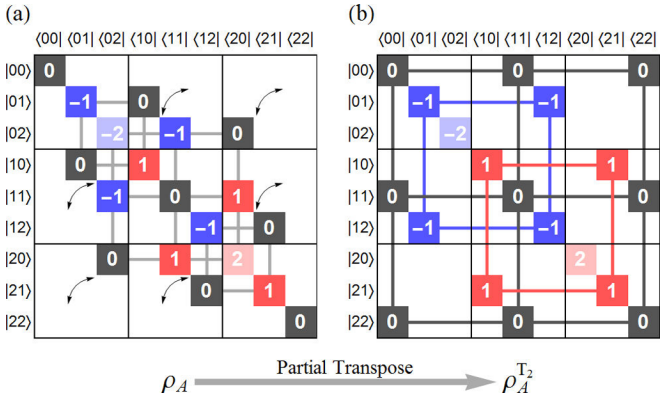

FIG. 1. Schematic block structure of density matrices in the basis of $|N_1 N_2\rangle$ with blocks labeled by $Q = N_1 - N_2^{T_2}$. (a) A density matrix ρ_A has a block structure with respect to $N_A = N_1 + N_2$ as shown by the thick lines. (b) Following a partial transposition, $\rho_A^{T_2}$ has a block structure determined by $Q = N_1 - N_2^{T_2}$ as shown by the thick lines. The partial transposition is indicated by the arrows in (a) and relates the blocks according to Eq. (12); for a specific example of these matrices see Eqs. (3) and (5).

entanglement entropies of many-body states in cold atoms, a recent work [11] showed that the same experimental protocol can be simply generalized to measure the Rényi negativity. Here we demonstrate that a similar protocol naturally allows one to measure separately the contributions to negativity from each symmetry sector.

The imbalance decomposition of negativity is also compatible with the elegant field theory methods that were applied to compute the total negativity of critical one-dimensional (1D) systems [12–16]. These computations are based on the replica trick approach, connecting the Rényi negativities with the partition function of the theory on an n-sheeted Riemann surface connected via crisscross escalators (see Fig. 3). Interestingly, a proper insertion of an Aharonov-Bohm-like flux into this n-sheeted Riemann surface [28,33–36] can be used to obtain universal predictions for the imbalance-resolved negativity. We show that these contributions share the same distribution as that of the charge difference between subsystems A_1 and A_2. We numerically test our field theory calculations for free fermions [26] by mapping the partial transposed density matrix to a sum of two Gaussian density matrices.

The plan of the paper is as follows. In Sec. II we begin by motivating our work by a simple example. As illustrated in Fig. 1, while number conservation is reflected by a block-diagonal structure of the density matrix, the operation of partial transposition mixes up these blocks; however, a new block structure is seen to emerge in terms of the imbalance operator Q. We proceed by a general definition of the imbalance operator and the associated decomposition of the negativity. In Sec. III we present an experimental protocol that enables measurements of the resolved Rényi negativities $[R_n]_Q$. In Sec. IV we focus on critical 1D systems and generalize conformal field theory (CFT) methods to derive a general result for the partition of the entanglement negativity. We then test our field theory results by performing an exact numerical calculation for a free system. Finally, a summary is provided in Sec. V.

II. IMBALANCE ENTANGLEMENT

In this section we provide a general definition of the symmetry resolution of entanglement negativity, referred to as imbalance entanglement. The key delicate issue to be addressed is the operation of *partial transposition* of the density matrix, which is best demonstrated by a simple example.

A. Intuitive example

In order to illustrate how symmetry is reflected in a block structure of the density matrix after partial transposition, it is beneficial to begin with the simplest example. Consider a single particle located in one out of three boxes A_1, A_2, and B. It is described by a pure state $|\Psi\rangle = \alpha|100\rangle + \beta|010\rangle + \gamma|001\rangle$. The reduced density matrix for subsystem $A = A_1 \cup A_2$ is $\rho_A = \mathrm{Tr}_B|\Psi\rangle\langle\Psi| = |\gamma|^2|00\rangle\langle 00| + (\alpha|10\rangle + \beta|01\rangle)(\alpha^*\langle 10| + \beta^*\langle 01|)$, whose matrix representation is given by

$$\rho_A = \left(\begin{array}{cc|cc} |\gamma|^2 & 0 & 0 & 0 \\ 0 & |\beta|^2 & \alpha^*\beta & 0 \\ \hline 0 & \beta^*\alpha & |\alpha|^2 & 0 \\ 0 & 0 & 0 & 0 \end{array}\right), \tag{3}$$

in the basis of $\{|00\rangle, |01\rangle, |10\rangle, |11\rangle\}$. This matrix has a block-diagonal structure with respect to the total occupation $N_A = N_1 + N_2$,

$$\rho_A \cong (|\gamma|^2)_{N_A=0} \oplus \begin{pmatrix} |\beta|^2 & \alpha^*\beta \\ \beta^*\alpha & |\alpha|^2 \end{pmatrix}_{N_A=1} \oplus (0)_{N_A=2}. \tag{4}$$

Let us turn our attention to the partially transposed density matrix $\rho_A^{T_2}$. It is obtained by transposing only the states of subsystem A_2 i.e., $|N_1 N_2\rangle\langle N_1' N_2'| \mapsto |N_1 N_2'\rangle\langle N_1' N_2|$. This is equivalent to transposing the submatrices of ρ_A,

$$\rho_A^{T_2} = \left(\begin{array}{cc|cc} |\gamma|^2 & 0 & 0 & \alpha^*\beta \\ 0 & |\beta|^2 & 0 & 0 \\ \hline 0 & 0 & |\alpha|^2 & 0 \\ \beta^*\alpha & 0 & 0 & 0 \end{array}\right). \tag{5}$$

The negativity spectrum for $\rho_A^{T_2}$ is easily found to be $\{|\alpha|^2, \frac{1}{2}|\gamma|^2 \pm \sqrt{\frac{1}{4}|\gamma|^4 + |\alpha\beta|^2}, |\beta|^2\}$ and contains only one negative eigenvalue $\mathcal{N} = |\frac{1}{2}|\gamma|^2 - \sqrt{\frac{1}{4}|\gamma|^4 + |\alpha\beta|^2}|$. Importantly, one may notice that $\rho_A^{T_2}$ has a block-matrix structure. We label the blocks according to the occupation imbalance $Q = N_1 - N_2$ of their diagonal elements,

$$\rho_A^{T_2} \cong (|\alpha|^2)_{Q=1} \oplus \begin{pmatrix} |\gamma|^2 & \alpha^*\beta \\ \beta^*\alpha & 0 \end{pmatrix}_{Q=0} \oplus (|\beta|^2)_{Q=-1}. \tag{6}$$

Here $N_1 - N_2 = 1$ corresponds to $\{|10\rangle\}$, $N_1 - N_2 = 0$ corresponds to $\{|00\rangle, |11\rangle\}$, and $N_1 - N_2 = -1$ corresponds to $\{|01\rangle\}$. This decomposition partitions the negativity spectrum $\{|\alpha|^2\} \cup \{\frac{1}{2}|\gamma|^2 \pm \sqrt{\frac{1}{4}|\gamma|^4 + |\alpha|^2|\beta|^2}\} \cup \{|\beta|^2\}$. As we henceforth show, this partitioning of the negativity spectrum goes beyond this example and is applicable to the general case.

B. General definition

One may define an imbalance partition with respect to any extensive operator $\hat{O}_{(A_1\cup A_2)\cup B} = \hat{O}_1 + \hat{O}_2 + \hat{O}_B$. For simplicity we focus on the case of a conserved total particle number $\hat{N}_{(A_1\cup A_2)\cup B} = \hat{N}_1 + \hat{N}_2 + \hat{N}_B$. Let us explore the consequences of this conservation law. It is reflected in the relation $[\rho_A, \hat{N}_A] = 0$ satisfied by the reduced density matrix $\rho_A = \mathrm{Tr}_B \rho$ (e.g., a thermal state $\rho_A \propto e^{-\beta \hat{H}}$). Partially transposing this commutation relation yields

$$\left[\rho_A^{\mathrm{T}_2}, \hat{N}_1 - \hat{N}_2^{\mathrm{T}_2}\right] = 0. \tag{7}$$

This commutativity elicits a block-matrix decomposition

$$\rho_A^{\mathrm{T}_2} = \bigoplus_Q \left[\rho_A^{\mathrm{T}_2}\right]_Q, \quad \hat{Q} \equiv \hat{N}_1 - \hat{N}_2^{\mathrm{T}_2}, \tag{8}$$

where Q are the eigenvalues of $\hat{Q}$. It is easily verified that this resolution is basis independent, i.e., that the spectrum of $[\rho_A^{\mathrm{T}_2}]_Q$ is invariant to local basis transformations $\hat{O} \mapsto (\hat{U}_1^\dagger \hat{U}_2^\dagger)\hat{O}(\hat{U}_1 \hat{U}_2)$ for all transformations $\hat{U}_\alpha$ acting only in regions A_α. The negativity spectrum $\{\lambda_i\}$ of $[\rho_A^{\mathrm{T}_2}]$ may thus be decomposed $\{\lambda_i\} = \bigcup_Q \{\lambda_{i_Q}\}$ into spectra $\{\lambda_{i_Q}\}$ of $[\rho_A^{\mathrm{T}_2}]_Q$ such that the overall entanglement negativity is resolved into contributions from distinct imbalance sectors

$$\mathrm{Tr}\left|\rho_A^{\mathrm{T}_2}\right| = \sum_Q \mathrm{Tr}\left\{\hat{P}_Q \left|\rho_A^{\mathrm{T}_2}\right|\right\} = \sum_Q \mathrm{Tr}\left|\left[\rho_A^{\mathrm{T}_2}\right]_Q\right|, \tag{9}$$

where $\hat{P}_Q$ is the projector to the subspace of eigenvalue Q of the operator $\hat{Q}$. Similarly, the Rényi negativity is decomposed as $R_n = \sum_Q [R_n]_Q$, where

$$[R_n]_Q \equiv \mathrm{Tr}\left\{\hat{P}_Q \left(\rho_A^{\mathrm{T}_2}\right)^n\right\} = \mathrm{Tr}\left\{\left(\left[\rho_A^{\mathrm{T}_2}\right]_Q\right)^n\right\}. \tag{10}$$

Generalizing the example from the preceding section, we write the density matrix as

$$\rho_A = \sum_{\{N\},\{i\}} |N_1\rangle^{i_1} |N_2\rangle^{i_2} [\rho_A]^{i_1,i_2;i_1',i_2'}_{N_1,N_2;N_1',N_2'} \langle N_1'|^{i_1'} \langle N_2'|^{i_2'}, \tag{11}$$

where $\{|N_\alpha\rangle^1, |N_\alpha\rangle^2, \dots\}$ span the Hilbert space of A_α with particle number N_α ($\alpha \in \{A_1, A_2\}$). Charge conservation implies that ρ_A commutes with $\hat{N}_1 + \hat{N}_2$. This leads to a block structure of ρ_A with $N_1 + N_2 = N_1' + N_2'$. This block structure of the density matrix is illustrated in the Fig. 1(a). We now wish to see which of these blocks contribute to each imbalance sector.

The block structure of ρ_A with $N_1 + N_2 = N_1' + N_2'$ allows us to identify $Q = N_1 - N_2' = N_2 - N_1'$ and assign a specific value of Q to each block, as marked inside the squares ($N_1, N_2; N_1', N_2'$ blocks) in Fig. 1(a). For example, the coherence term $\beta^*\alpha$ in Sec. II A corresponds to $|N_1 N_2\rangle\langle N_1' N_2'| = |10\rangle\langle 01|$ and hence to $Q = 0$.

Now consider the partially transposed density matrix. The blocks of the original density matrix that contribute to $[\rho_A^{\mathrm{T}_2}]_Q$ for a given Q are

$$\left[\rho_A^{\mathrm{T}_2}\right]^{\{i\}}_{N_1,N_1-Q;N_2+Q,N_2} = [\rho_A]^{\{i\}}_{N_1,N_2;N_2+Q,N_1-Q}. \tag{12}$$

As can be seen in Fig. 1(b), these blocks reorganize into a diagonal-block structure labeled by Q after partial transposition. Staring at diagonal blocks of ρ_A, i.e., $(N_1, N_2) = (N_1', N_2')$, we see that $Q \leftrightarrow N_1 - N_2$ is just the charge imbalance between the two subsystems, motivating the term "imbalance decomposition" [note, though, that the density matrix also contains nondiagonal blocks where $(N_1, N_2) \neq (N_1', N_2')$ and that the blocks that contribute to the Q imbalance sectors are precisely those in Eq. (12)].

III. PROTOCOL FOR EXPERIMENTAL DETECTION

In the preceding section we identified the imbalance operator Q according to which the partially transposed density matrix admits a block-diagonal form, allowing us to decompose the negativity spectrum. In this section we show that a measurement of the individual imbalance contributions to the Rényi negativities can be performed within an existing experimental setup. For this purpose we adopt protocols which have been recently implemented in an experiment measuring entanglement entropy [32]. Specifically, in order to measure the resolved Rényi negativity $[R_n]_Q$ we will build on a recently proposed protocol [11] based on Ref. [31], designed specifically to measure the total Rényi negativity R_n.

We begin this section by presenting the basic idea of the protocol for measuring entanglement entropy and then progressively show how the entanglement entropy and the negativity can be measured and partitioned according to symmetry sectors. The impatient reader interested directly in the protocol may skip to Sec. III E.

A. Key idea and the shift operator

The starting point for the entanglement measurement protocols under consideration is a preparation of n copies of the many-body system. If, for instance, the original Hilbert space under consideration corresponds to that of a 1D chain as depicted in Fig. 2(a), then one extends the Hilbert space into a product of n such Hilbert spaces describing n identical chains as described in Fig. 2(b). In this space one wishes to prepare the n-copy state $\rho_A^{\otimes n}$ of the original state ρ_A. This can be achieved [32] using optical lattices in cold-atom systems, where one simulates the same Hamiltonian on the n initially decoupled identical chains.

One then defines an operator in the extended Hilbert space, shifting between the quantum states of the copies in region A. It is simpler to restrict our attention to region A from now on in this section. Explicitly, we denote a basis of states on the n-copy Hilbert space of region A by $|\psi^1, \psi^2, \dots, \psi^n\rangle$ and the shift operator $\hat{S}$ is defined via

$$\hat{S}|\psi^1, \psi^2, \dots, \psi^n\rangle = |\psi^n, \psi^1, \dots, \psi^{n-1}\rangle. \tag{13}$$

The key relation used in the protocol is that the Rényi entropies S_n satisfy

$$S_n \equiv \mathrm{Tr}\left\{\rho_A^n\right\} = \mathrm{Tr}\left\{\hat{S}\rho_A^{\otimes n}\right\}, \tag{14}$$

i.e., the expectation value of the shift operator in the n-copy state equals the desired Rényi entropy [31]. As described in detail in the next section, the protocol proceeds by a proper manipulation of the n-copy system via a transformation between the copies [see Fig. 2(c)], followed by site-resolved measurements [see Fig. 2(d)]. The combination of the latter

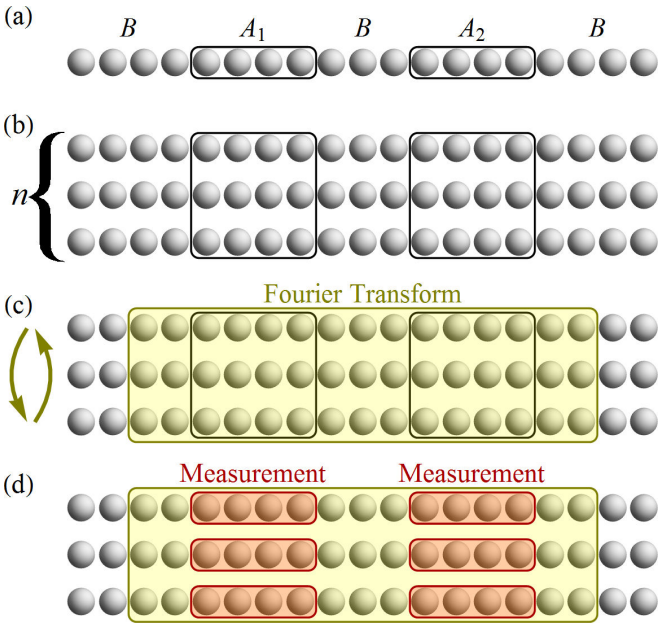

FIG. 2. Depiction of the experimental protocol to measure the imbalance-resolved Rényi negativity. (a) The system is tripartitioned into regions A_1, A_2, and B. (b) n copies of the system are prepared. (c) A copy-space Fourier transform is performed on a region containing A_1 and A_2. (d) The $N^k_{A_1}$ and $N^k_{A_2}$ are measured in regions A_1 and A_2 ($k = 1, \ldots, n$), and $q = \frac{1}{n}\sum_k (N^k_{A_1} - N^k_{A_2})$ and $r_n = \exp\{\sum_k \frac{2\pi i}{n} k(N^k_{A_1} - N^k_{A_2})\}$ of Eq. (34) are calculated. The contribution of imbalance sector Q to the Rényi negativity is then given by the average over $\delta_{Q,q} \times r_n$.

two is designed precisely to implement a measurement of the expectation value of the shift operator in the n-copy state.

B. Measuring Rényi entropy

Before turning to negativity, it is convenient to introduce notation and show that the protocol just described indeed can measure the expectation value of the shift operator and hence the Rényi entropy. Consider a general bosonic state in the occupation basis

$$|\vec{m}^1, \vec{m}^2, \ldots, \vec{m}^n\rangle = \prod_{k=1}^{n}\prod_{i\in A} \frac{\left([\hat{a}^\dagger]_i^k\right)^{m_i^k}}{\sqrt{m_i^k!}}|0\rangle. \tag{15}$$

Here the index k runs over the n copies and i runs over all sites in region A. We then perform a Fourier transform in the $(k = 1, \ldots, n)$-copy space

$$\hat{F}[\hat{a}^\dagger]_i^k \hat{F}^\dagger = \frac{1}{\sqrt{n}}\sum_{\ell=1}^{n} \omega^{k\ell}[\hat{a}^\dagger]_i^\ell, \tag{16}$$

where $\omega = e^{2\pi i/n}$, such that

$$\hat{F}|\vec{m}^1, \ldots, \vec{m}^n\rangle = \prod_{k,i} \frac{\left(\frac{1}{\sqrt{n}}\sum_\ell \omega^{k\ell}[\hat{a}^\dagger]_i^\ell\right)^{m_i^k}}{\sqrt{m_i^k!}}|0\rangle. \tag{17}$$

Let us look at the operator

$$\hat{U} \equiv \omega^{\sum_{k=1}^n k\hat{N}^k}, \tag{18}$$

where $\hat{N}^k = \sum_{i\in A}[\hat{a}^\dagger]_i^k[\hat{a}]_i^k$ is the total particle number operator in region A in the kth copy. It satisfies $\hat{U}[\hat{a}^\dagger]_i^k = \omega^k[\hat{a}^\dagger]_i^k\hat{U}$. Using this relation, when acting on the Fourier transformed state this operator gives

$$\begin{aligned}
&\hat{U}\hat{F}|\vec{m}^1, \vec{m}^2, \ldots, \vec{m}^n\rangle \\
&= \prod_{k,i}\frac{1}{\sqrt{m_i^k!}}\left(\frac{1}{\sqrt{n}}\sum_\ell \omega^{(k+1)\ell}[\hat{a}^\dagger]_i^\ell\right)^{m_i^k}|0\rangle \\
&= \prod_{k,i}\frac{1}{\sqrt{m_i^k!}}\left(\frac{1}{\sqrt{n}}\sum_\ell \omega^{k\ell}[\hat{a}^\dagger]_i^\ell\right)^{m_i^{k-1}}|0\rangle \\
&= \hat{F}|\vec{m}^n, \vec{m}^1, \ldots, \vec{m}^{n-1}\rangle = \hat{F}\hat{S}|\vec{m}^1, \ldots, \vec{m}^n\rangle.
\end{aligned} \tag{19}$$

In exchanging the order of creation operators we have used the bosonic commutation relations. Since this equation holds for all states $|\vec{m}^1, \vec{m}^2, \ldots, \vec{m}^n\rangle$, one has

$$\hat{F}^\dagger\hat{U}\hat{F} = \hat{S}. \tag{20}$$

This operator identity implies that measurements of $\hat{U} = \omega^{\sum_{k=1}^n k\hat{N}^k}$ on the Fourier transformed system yields the expectation value of $\hat{S}$, hence, by Eq. (14), if the system is in an n-copy state, this gives the Rényi entropy $S_n = \mathrm{Tr}\{\rho_A^n\}$.

In other words, defining the set of commuting occupancies of region A of the various copies after the Fourier transform by $\{\tilde{N}\}$, where $\hat{\tilde{N}}^k = \hat{F}^\dagger\hat{N}^k\hat{F}$, the experiment simply performs a measurement in this new occupation basis and computes a function $f(\{\tilde{N}\})$ of the outcomes $\{\tilde{N}\}$ given by

$$f(\{\tilde{N}\}) \equiv \omega^{\sum_{k=1}^n k\tilde{N}^k}. \tag{21}$$

Operationally, the operational identity (20) is equivalent to $\hat{f}(\{\tilde{N}\}) = \omega^{\sum_k k\hat{\tilde{N}}^k} = \hat{S}$. Thus, we can describe the experimental protocol via

$$\mathrm{Tr}\left\{\rho_A^{\otimes n}\hat{f}(\{\tilde{N}\})\right\} = \mathrm{Tr}\left\{\rho_A^{\otimes n}\hat{S}\right\}. \tag{22}$$

The left-hand side describes the measurement performed in the $\{\tilde{N}^k\}$ basis and the right-hand side is the desired quantity.

We note that the choice of a function $f(\{\tilde{N}\})$ is not unique. Since the matrix element of the shift operator vanishes except if $N^1 = N^2 = \cdots = N^n$, one can replace the function f with $\omega^{\sum_{k=1}^n (k+m)\tilde{N}^k}$, and its average in the n-copy state is invariant with respect to the integer m. In fact, one can use this invariance as an experimental test of the operation of the protocol. In the experiment [32] for $n = 2$, for example, this amounts to the possibility to measure the parity either in copy 1 or in copy 2, which must yield the same average result.

C. Measuring charge-resolved Rényi entropy

Using this notation, it becomes simple to demonstrate the protocol for measuring the charge-resolved Rényi entropy [28]. In the presence of a conserved number of particles N_A, the general density matrix can be written, using the same notation as in Eq. (11),

$$\rho_A = \sum_N \sum_{i,i'} |N\rangle^i [\rho_A]_N^{ii'} \langle N|^{i'}. \tag{23}$$

Here $|N\rangle^i$ and $|N\rangle^{i'}$ are different states having the same total number of particles N. Therefore, the n-copy density matrix can be written, using a superindex $|\mathbf{N}\rangle \equiv |N^1, N^2, \ldots, N^n\rangle^{i^1,i^2,\ldots,i^n}$, as

$$\rho_A^{\otimes n} = \sum_{\mathbf{N},\mathbf{N}'} [\rho_A]_{\mathbf{N},\mathbf{N}'} |\mathbf{N}\rangle\langle\mathbf{N}'|, \tag{24}$$

where $N^k = N'^k$ $(k = 1, \ldots, n)$. We are now interested in measuring the contribution of the charge $N_A = N$ block of the density matrix $[\rho_A]_N = \sum_{i,i'} |N\rangle^i [\rho_A]_N^{ii'} \langle N|^{i'}$ to the Rényi entropy [28]. This quantity $[S_n]_N = \mathrm{Tr}\{([\rho_A]_N)^n\}$ equals the expectation value of the shift operator in the n-copy state obtained by $[\rho_A]_N^{\otimes n}$. This may be measured after the Fourier transformation by calculating the function

$$f_{N_A}(\{\tilde{N}\}) \equiv \delta_{N_A, \frac{1}{n}\sum_{k=1}^n \tilde{N}^k} \times \omega^{\sum_{k=1}^n k\tilde{N}^k}. \tag{25}$$

To prove this statement we start with

$$\mathrm{Tr}\left\{\rho_A^{\otimes n} \hat{f}_{N_A}(\{\tilde{N}\})\right\} = \sum_{\mathbf{N},\mathbf{N}'} [\rho_A]_{\mathbf{N},\mathbf{N}'} \langle\mathbf{N}'|\hat{f}_{N_A}(\{\tilde{N}\})|\mathbf{N}\rangle. \tag{26}$$

Since the sum of the particle number is invariant under the Fourier transformation $\sum_{k=1}^n \tilde{N}^k = \sum_{k=1}^n N^k$, Eq. (26) equals

$$\begin{aligned}&\sum_{\mathbf{N},\mathbf{N}'} \left(\delta_{N_A, \frac{1}{n}\sum_k N^k}\right) [\rho_A]_{\mathbf{N},\mathbf{N}'} \langle\mathbf{N}'|\omega^{\sum_k k\tilde{N}^k}|\mathbf{N}\rangle \\ &\quad = \sum_{\mathbf{N},\mathbf{N}'} \left(\delta_{N_A, \frac{1}{n}\sum_k N^k}\right) [\rho_A]_{\mathbf{N},\mathbf{N}'} \langle\mathbf{N}'|\hat{S}|\mathbf{N}\rangle,\end{aligned} \tag{27}$$

where the last equality uses Eq. (20). Crucially, the matrix element of the shift operator vanishes except if $N^1 = N^2 = \cdots = N^n$, namely, it is proportional to $\prod_{k,k'} \delta_{N^k,N^{k'}}$. Thus, we conclude that

$$\begin{aligned}\mathrm{Tr}\left\{\rho_A^{\otimes n} \hat{f}_{N_A}(\{\tilde{N}\})\right\} &= \sum_{\mathbf{N},\mathbf{N}'} \left(\prod_k \delta_{N_A,N^k}\right) [\rho_A]_{\mathbf{N},\mathbf{N}'} \langle\mathbf{N}'|\hat{S}|\mathbf{N}\rangle \\ &= \mathrm{Tr}\left\{[\rho_A]_{N_A}^{\otimes n}\hat{S}\right\} = [S_n]_{N_A}.\end{aligned} \tag{28}$$

D. Measuring negativity

Switching to the Rényi negativity, one defines a twisted shift operator $\hat{T} = \hat{S}_{A_1}\hat{S}_{A_2}^{-1}$ on the n-copy Hilbert space of region A such that

$$\hat{T}\left|\begin{matrix}\vec{m}_{A_1}^1, \ldots, \vec{m}_{A_1}^n \\ \vec{m}_{A_2}^1, \ldots, \vec{m}_{A_2}^n\end{matrix}\right\rangle = \left|\begin{matrix}\vec{m}_{A_1}^n, \vec{m}_{A_1}^1, \ldots, \vec{m}_{A_1}^{n-1} \\ \vec{m}_{A_2}^2, \ldots, \vec{m}_{A_2}^n, \vec{m}_{A_2}^1\end{matrix}\right\rangle. \tag{29}$$

Here this basis specifies the occupations $\vec{m}_{A_1}^1, \ldots, \vec{m}_{A_1}^n$ on the n copies of subsystem A_1 as well as the occupations $\vec{m}_{A_2}^1, \ldots, \vec{m}_{A_2}^n$ on the n copies of subsystem A_2. In analogy to Eq. (14), the Rényi negativity is given by the expectation value of this shift operator in the n-copy state [11],

$$R_n = \mathrm{Tr}\left\{\left(\rho_A^{T_2}\right)^n\right\} = \mathrm{Tr}\left\{\hat{T}\rho_A^{\otimes n}\right\}. \tag{30}$$

To proceed with the measurement of the expectation value of this shift operator in the n-copy state, we use the same Fourier transform on all sites as in Eq. (16), but generalize the definition of the $\hat{U}$ operator in Eq. (18) to

$$\hat{U} \equiv \omega^{\sum_{k=1}^n k\left(\hat{N}_{A_1}^k - \hat{N}_{A_2}^k\right)}. \tag{31}$$

Here $N_{A_\alpha}^k$ is the total particle number operator in subsystem A_α of the kth copy, i.e., $N_{A_1}^k = \sum_{i\in A_1} m_i^k$ and $N_{A_2}^k = \sum_{i\in A_2} m_i^k$. Following the same steps as in Eq. (19), we readily obtain the relation

$$\hat{T} = \hat{F}^\dagger \omega^{\sum_{k=1}^n k(\hat{N}_{A_1}^k - \hat{N}_{A_2}^k)} \hat{F}. \tag{32}$$

Thus, the physical protocol first consists of a unitary Hamiltonian evolution depicted in Fig. 2(c) which implements [31] the Fourier transformation $\hat{F}$. Then, as in Fig. 2(d), we perform a measurement of the total occupancies $N_{A_1}^k$ and $N_{A_2}^k$ in each region A_1 and A_2 and in each copy, from which

$$f^{\mathrm{neg}}(\{N\}) \equiv \omega^{\sum_{k=1}^n k(N_{A_1}^k - N_{A_2}^k)} \tag{33}$$

can be computed, and averaged over many realizations to obtain the total Rényi negativity.

E. Measuring imbalance-resolved negativity

We are now ready to provide a protocol to measure the symmetry-resolved negativity. We begin with a step-by-step description of the protocol, followed by an outline of the proof which relies on the previous sections.

Our protocol to measure the Rényi negativity $[R_n]_Q$ for bosons consists of the following steps (see Fig. 2).

(i) Prepare n copies of the desired system.

(ii) Decouple the sites within each copy and perform a Fourier transform on every site between the copies. This is achieved by a unitary Hamiltonian evolution which implements Eq. (16).

(iii) Perform a measurement of the total particle number $N_{A_1}^k$ in subsystem A_1 and of $N_{A_1}^k$ in A_2 for each copy $k = 1 \ldots n$.

(iv) Calculate

$$q \equiv \frac{1}{n}\sum_{k=1}^n \left(N_{A_1}^k - N_{A_2}^k\right), \quad r_n \equiv e^{\frac{2\pi i}{n}\sum_{k=1}^n k(N_{A_1}^k - N_{A_2}^k)}. \tag{34}$$

To obtain the value of $[R_n]_Q$ one must repeat this procedure and average over a quantity which is equal to r_n if q equals the required imbalance sector $q = Q$ and is 0 otherwise. In other words,

$$[R_n]_Q = \mathrm{Tr}\left\{\rho_A^{\otimes n} \hat{f}_Q^{\mathrm{neg}}(\{\tilde{N}\})\right\}, \tag{35}$$

where the right-hand side reflects the measurement protocol in the occupation basis $\tilde{N}$ after the Fourier transformation and

$$f_Q^{\mathrm{neg}}(\{N\}) \equiv \delta_{Q, \frac{1}{n}\sum_k (N_{A_1}^k - N_{A_2}^k)} \times e^{\frac{2\pi i}{n}\sum_k k(N_{A_1}^k - N_{A_2}^k)}. \tag{36}$$

A few remarks about our protocol are in order. First, it is not necessary to perform the Fourier transform exclusively on the sites of subsystem A. Instead, one needs only to perform a Fourier transform on any region C of the system that contains region A. This simplification allows for experimental flexibility. Second, if one measures the total particle numbers $N_{A_1}^k$ and $N_{A_2}^k$ in subsystems A_1 and A_2 by performing occupation measurements on every site, one can immediately get the Rényi negativity for all partitions of A, i.e., for all $A_1' \cup A_2' = A \subseteq C$. Third, by evaluating Q, the occupancy measurements automatically decompose the entanglement negativity into imbalance sectors.

We also note that we have restricted our analysis to bosons. The case of fermions was addressed for the second Rényi entropy in Ref. [37] and we leave generalizations to future work [38]. In addition, while we only discussed the $n \geqslant 2$ Rényi entropies and negativities, one may use the methods in Ref. [11] to access the corresponding entanglement entropy or negativity obtained by analytic continuation and taking the limit of $n \to 1$.

The proof of Eq. (35) follows from the relation $\mathrm{Tr}\{[\rho_A]_Q^{\otimes n}\hat{T}\} = \mathrm{Tr}\{\rho_A^{\otimes n}\hat{f}_Q^{\mathrm{neg}}(\{\tilde{N}\})\}$; the left-hand side is the expectation value of the twisted shift operator in the n-copy state of the imbalance-Q sector $[\rho_A]_Q \equiv ([\rho_A^{\mathrm{T}_2}]_Q)^{\mathrm{T}_2}$, which satisfies $[R_n]_Q = \mathrm{Tr}\{[\rho_A]_Q^{\otimes n}\hat{T}\}$. In order to show this relation we write a general state using the superindex notation

$$|\mathbf{N}\rangle \equiv \left|N_{A_1}^1,\ldots,N_{A_1}^n\right\rangle^{i_{A_1}^1,\ldots,i_{A_1}^n}\left|N_{A_2}^1,\ldots,N_{A_2}^n\right\rangle^{i_{A_2}^1,\ldots,i_{A_2}^n}, \quad (37)$$

where $\{|N_{A_\alpha}^k\rangle^1, |N_{A_\alpha}^k\rangle^2, |N_{A_\alpha}^k\rangle^3,\ldots\}$ span the Hilbert space of subsystem A_α in copy k. We proceed exactly along the lines of Eqs. (26)–(28) and hence only provide key remarks. We use the fact that the total number of particles in each region A_1 and A_2 remains invariant under the Fourier transformation $\sum_{k=1}^n \tilde{N}_{A_\alpha}^k = \sum_{k=1}^n N_{A_\alpha}^k$. This allows us to extract the δ function operator from the matrix element $\langle\mathbf{N}'|\delta_{Q,(1/n)\sum_{k=1}^n(\tilde{N}_{A_1}^k-\tilde{N}_{A_2}^k)}e^{(2\pi i/n)\sum_{k=1}^n k(\tilde{N}_{A_1}^k-\tilde{N}_{A_2}^k)}|\mathbf{N}\rangle$. Finally, we use the relation (32) to obtain a matrix element of the twisted shift operator $\langle\mathbf{N}'|\hat{T}|\mathbf{N}\rangle$. The twisted shift operator acts as

$$\hat{T}\left|\begin{matrix}N_{A_1}^1,\ldots,N_{A_1}^n\\ N_{A_2}^1,\ldots,N_{A_2}^n\end{matrix}\right\rangle^{\{i\}} = \left|\begin{matrix}N_{A_1}^n,N_{A_1}^1,\ldots,N_{A_1}^{n-1}\\ N_{A_2}^2,\ldots,N_{A_2}^n,N_{A_2}^1\end{matrix}\right\rangle^{\{i\}}. \quad (38)$$

States contributing to this matrix element satisfy $N_{A_1}'^k = N_{A_1}^{k-1}$ and $N_{A_2}'^k = N_{A_2}^{k+1}$. In addition, charge conservation implies $N_{A_1}^k + N_{A_2}^k = N_{A_1}'^k + N_{A_2}'^k$. This set of equations allows us to define

$$\begin{aligned} Q \equiv N_{A_1}^1 - N_{A_2}^2 &= N_{A_1}^n - N_{A_2}^1 \\ &= N_{A_1}^{n-1} - N_{A_2}^n = \cdots = N_{A_1}^2 - N_{A_2}^3. \end{aligned} \quad (39)$$

By summing all these equations, we get

$$Q = \frac{1}{n}\sum_{k=1}^n\left(N_{A_1}^k - N_{A_2}^k\right) = \frac{1}{n}\sum_{k=1}^n(\tilde{N}_{A_1}^k - \tilde{N}_{A_2}^k). \quad (40)$$

By observing Eq. (39) we can see that the states which contribute are exactly the blocks of the original density matrix that satisfy Eq. (12); these precisely form the imbalance-Q sector.

IV. FIELD THEORY ANALYSIS

Having shown the possibility to experimentally measure the separation of negativity into symmetry sectors, we now study 1D critical systems where general results for this quantity can be readily obtained. In such 1D critical systems the entanglement entropy shows the famous logarithmic scaling

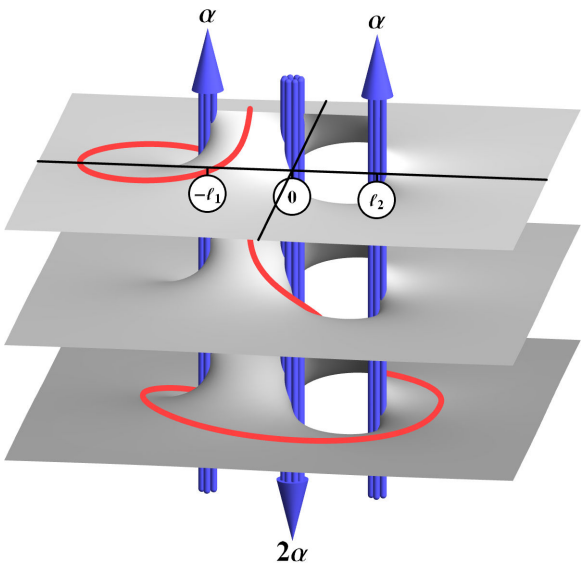

FIG. 3. Schematic representation of the Rényi negativity $\mathrm{Tr}\{(\rho_A^{\mathrm{T}_2})^n\}$ as an n-sheet Riemann surface with $A_1 = [-\ell_1, 0]$ and $A_2 = [0, \ell_2]$. The phase factor $\exp\{i\alpha(N_1 - N_2^{\mathrm{T}_2})\}$ is implemented by flux insertions $\mathcal{V}_\alpha(-\ell_1)\mathcal{V}_{-2\alpha}(0)\mathcal{V}_\alpha(\ell_2)$ and represented by the vertical arrows. The winding line serves only as a visual aid.

with the subsystem size $S = \frac{c}{3}\log(\ell_A) + \mathrm{const}$, which can be decomposed into charge sectors [28] $S = \sum_{N_A}[S]_{N_A}$; the contributions $[S]_{N_A}$ were found [28] to share the same distributions as the charge N_A in region A [39]. We will now address a similar question for the negativity and its imbalance decomposition.

Similar to the entanglement entropy scaling result, the negativity of two subsystems consisting of two adjacent intervals A_1 and A_2, of lengths ℓ_1 and ℓ_2, out of an infinite system in the ground state, has also been studied in the scaling limit. It acquires a universal form [12] $\mathrm{Tr}|\rho_A^{\mathrm{T}_2}| = R_{n_e\to 1} \propto (\frac{\ell_1\ell_2}{\ell_1+\ell_2})^{c/4}$, depending only on the central charge c. We will decompose this result into imbalance sectors. We note that although the case of nonadjacent intervals may be treated using similar methods, it is more technically involved and so we do not explicitly address it in this section.

We begin by briefly recapitulating the computation method of negativity based on Ref. [12] using CFT. We note that these field theory methods are closely related in spirit to the n-copy construction of the system discussed in the preceding section. In field theory [12], the Rényi negativity is treated as a partition function of an n-sheet Riemann surface depicted in Fig. 3. It is found to be determined by the three-point correlation function of local "twist" fields,

$$R_n = \mathrm{Tr}\left\{\left(\rho_A^{\mathrm{T}_2}\right)^n\right\} = \left\langle\mathcal{T}_n(-\ell_1)\tilde{\mathcal{T}}_n^2(0)\mathcal{T}_n(\ell_2)\right\rangle. \quad (41)$$

The twist fields $\mathcal{T}_n$ generate the n-sheet Riemann surface depicted in Fig. 3 and have scaling dimensions

$$\Delta_{\mathcal{T}_n} = \frac{c(n-1/n)}{24}, \quad \Delta_{\mathcal{T}_{n_o}^2} = \Delta_{\mathcal{T}_{n_o}}, \quad \Delta_{\mathcal{T}_{n_e}^2} = 2\Delta_{\mathcal{T}_{n_e/2}}. \quad (42)$$

Here we split the results for the scaling dimension of the squared twist field for even ($n = n_e$) and odd ($n = n_o$) cases.

Using these scaling dimensions, the desired three-point function is easily evaluated,

$$R_{n_o} \propto [\ell_1\ell_2(\ell_1+\ell_2)]^{-\frac{c}{12}(n_o-\frac{1}{n_o})}, \tag{43}$$

$$R_{n_e} \propto (\ell_1\ell_2)^{-\frac{c}{6}(\frac{n_e}{2}-\frac{2}{n_e})}(\ell_1+\ell_2)^{-\frac{c}{6}(\frac{n_e}{2}+\frac{1}{n_e})}, \tag{44}$$

$$\mathrm{Tr}\big|\rho_A^{\mathrm{T}_2}\big| = R_{n_e\to 1} \propto \left(\frac{\ell_1\ell_2}{\ell_1+\ell_2}\right)^{\frac{c}{4}}. \tag{45}$$

We herein implement the negativity splitting of Eq. (9). To do so, we use the Fourier representation of the projection operator

$$\hat{P}_Q = \int_{-\pi}^{\pi}\frac{d\alpha}{2\pi}e^{-i\alpha Q}e^{i\alpha(\hat{N}_1-\hat{N}_2^{\mathrm{T}_2})}, \quad \sum_Q \hat{P}_Q = 1. \tag{46}$$

In the context of field theory, however, we treat the system in the continuum limit such that

$$\hat{P}_Q = \int_{-\infty}^{\infty}\frac{d\alpha}{2\pi}e^{-i\alpha Q}e^{i\alpha(\hat{N}_1-\hat{N}_2^{\mathrm{T}_2})}, \quad \int_{-\infty}^{\infty} dQ\,\hat{P}_Q = 1. \tag{47}$$

We now restrict our attention to a CFT of central charge $c = 1$ which is equivalent to 1D massless bosons and thus to Luttinger liquids (gapless interacting 1D fermions [40,41]). Applying the methods of Ref. [28], the phase factor $e^{i\alpha(\hat{N}_1-\langle\hat{N}_1\rangle)}$ may be implemented by two vertex operators $\mathcal{V}_\alpha$ at $z=-\ell_1$ and $\mathcal{V}_{-\alpha}$ at $z=0$. Moreover, within the CFT's geometrical basis, $\hat{N}$ is a real operator and thus $\hat{N}^{\mathrm{T}_2}=\hat{N}^*=\hat{N}$ and so a similar vertex operator insertion may account for $e^{-i\alpha(\hat{N}_2-\langle\hat{N}_2\rangle)}$. In general, such insertions may be done in any of the $k=1,\ldots,n$ sheets with different phases α_k, However, these vertex operators may be interpreted as a flux insertion, in which case gauge invariance implies that only the overall flux has physical implications. Indeed, using the techniques of Refs. [33,42], we show in Appendix A that this physical intuition holds and that the correlations depend only on the total flux $\alpha=\sum_{k=1}^n\alpha_k$. Considering a generic Luttinger liquid with parameter K, we find the scaling dimension of the fluxed twist operator $\mathcal{T}_n\mathcal{V}_\alpha$ to be [28]

$$\Delta_n(\alpha) = \frac{1}{24}\left(n-\frac{1}{n}\right)+\frac{K}{2n}\left(\frac{\alpha}{2\pi}\right)^2. \tag{48}$$

In terms of these fluxed twist operators, the negativities are also related to three-point functions

$$[R_n]_Q = \int_{-\infty}^{\infty}\frac{d\alpha}{2\pi}e^{-i\alpha(Q-\langle\hat{Q}\rangle)}R_n(\alpha), \tag{49}$$

$$\begin{aligned}R_n(\alpha) &= e^{-i\alpha\langle\hat{N}_1-\hat{N}_2^{\mathrm{T}_2}\rangle}\mathrm{Tr}\big\{e^{i\alpha(\hat{N}_1-\hat{N}_2^{\mathrm{T}_2})}\big(\rho_A^{\mathrm{T}_2}\big)^n\big\}\\ &= \big\langle(\mathcal{T}_n\mathcal{V}_\alpha)_{z=-\ell_1}\big(\tilde{\mathcal{T}}_n^2\mathcal{V}_{-2\alpha}\big)_{z=0}(\mathcal{T}_n\mathcal{V}_\alpha)_{z=\ell_2}\big\rangle.\end{aligned} \tag{50}$$

Using the scaling dimensions given in Eqs. (42) and (48), we evaluate

$$\frac{R_n(\alpha)}{R_n} \propto (\ell_1\ell_2)^{-\frac{4K}{n}(\frac{\alpha}{2\pi})^2}(\ell_1+\ell_2)^{\frac{2K}{n}(\frac{\alpha}{2\pi})^2}. \tag{51}$$

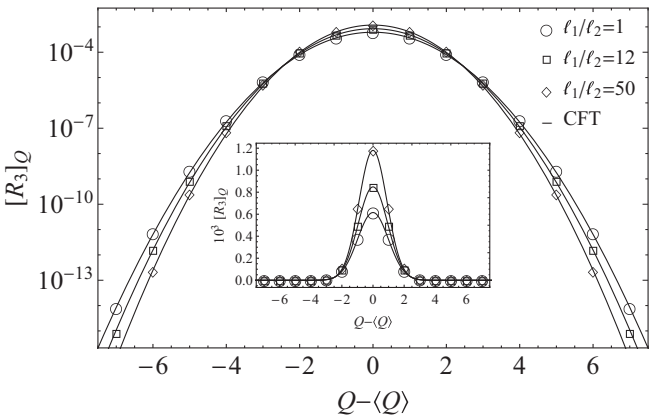

FIG. 4. Exact numerical calculations of $[R_3]_Q$ for a half-filled tight-binding chain of free fermions are displayed on a logarithmic scale and fitted to the CFT predictions (solid lines) of Eq. (52) with $K=1$. The inset shows the same data displayed on a linear scale. All graphs are for $\ell_1+\ell_2=4000a$ and infinite-length environment B.

Upon integration over α in Eq. (49) we obtain the result

$$\frac{[R_n]_Q}{R_n} = \sqrt{\frac{\pi n}{2K\ln\frac{\ell_1^2\ell_2^2}{(\ell_1+\ell_2)\Lambda^3}}}\exp\left(-\frac{n\pi^2(Q-\langle\hat{Q}\rangle)^2}{2K\ln\frac{\ell_1^2\ell_2^2}{(\ell_1+\ell_2)\Lambda^3}}\right), \tag{52}$$

$$\frac{\mathrm{Tr}\big|\big[\rho_A^{\mathrm{T}_2}\big]_Q\big|}{\mathrm{Tr}\big|\rho_A^{\mathrm{T}_2}\big|} = \left[\frac{[R_n]_Q}{R_n}\right]_{n_e\to 1}, \tag{53}$$

where $\Lambda\sim a\ll\ell$ is a short distance cutoff and a is the lattice spacing. These equations provide an analytic expression for the imbalance-resolved negativity and Rényi negativities which are numerically inaccessible for large systems.

One may simply cast the result for the negativity equations (52) and (53) as

$$\mathrm{Tr}\big|\big[\rho_A^{\mathrm{T}_2}\big]_Q\big| = \langle\hat{P}_{N_1-N_2=Q}\rangle\mathrm{Tr}\big|\rho_A^{\mathrm{T}_2}\big|. \tag{54}$$

It follows from the identity that $\mathrm{Tr}\,\hat{O}=\mathrm{Tr}\{\hat{O}^{\mathrm{T}_2}\}$, which leads to $[R_1]_Q=\langle\hat{P}_{N_1-N_2=Q}\rangle$ [see Eq. (55)]. This result signifies that the imbalance-resolved negativity depends only on the probability distribution function of the occupation imbalance N_1-N_2 itself, $\langle\hat{P}_{N_1-N_2=Q}\rangle$. The latter depends on the Luttinger parameter as seen in Eq. (52).

The expression for the $n=3$ Rényi negativity is numerically accessible and is used in the following section to validate our results (see Fig. 4).

Numerics

For adjacent intervals A_1 and A_2, one may use the Jordan-Wigner transformation to relate the entanglement of either hard-core bosons or a bosonic spin-half chain such as the XY model [43,44] to that of free fermions. This corresponds to the case of Luttinger parameter $K=1$, whereby we may use free-fermion methods to effectively calculate the negativities.

By generalizing the analysis of Refs. [26,45] and using the results of Refs. [46,47], we may study the Rényi negativity in any equilibrium free-fermion system with density matrix

$\rho \propto e^{-\beta \hat{H}}$ via a double-Gaussian representation. Specifically, we may calculate $\mathrm{Tr}\{e^{\hat{O}}(\rho_A^{\mathrm{T}_2})^n\}$ for any operator $\hat{O}$ that is quadratic in fermionic creation and annihilation operators (see Appendix B). To utilize these techniques, we use Eq. (46) with $\hat{O} = i\alpha(\hat{N}_1 - \hat{N}_2^{\mathrm{T}_2})$,

$$[R_n]_Q = \mathrm{Tr}\left\{\hat{P}_Q\left(\rho_A^{\mathrm{T}_2}\right)^n\right\} = \int_{-\pi}^{\pi} \frac{d\alpha}{2\pi} e^{-i\alpha Q} \mathrm{Tr}\left\{e^{i\alpha(\hat{N}_1 - \hat{N}_2^{\mathrm{T}_2})}\left(\rho_A^{\mathrm{T}_2}\right)^n\right\}. \quad (55)$$

Numerical results for $[R_3]_Q$ for free fermions at zero temperature are shown in Fig. 4 and are fitted to the CFT predictions of Eq. (52) with $K = 1$. Analyses for Λ/a of similar systems are known [39,48] to range between 0.1017 and 0.1033. Within the validity regime $\Lambda \ll \ell$, the functional dependence on Λ is negligible, and all values in the aforementioned range yield excellent fits to the data; the figure is plotted with $\Lambda/a = 0.1$. Further details about the numerical technique are given in Appendix B.

V. CONCLUSION AND OUTLOOK

We studied entanglement negativity in general many-body systems possessing a global conserved charge and found it to be decomposable into symmetry sectors. Interestingly, due to the partial transposition operation involved in the definition of negativity, the resulting operator that commutes with the partially transposed density matrix is not the total charge, but rather an imbalance operator which is essentially the particle number difference between two regions.

We have proposed an experimental protocol for the measurement of these contributions to the Rényi negativities using existing cold-atom technologies. While current cold-atom detection schemes [32] are based on measurements of the *parity* of the on-site occupation due to unavoidable two-atom molecule formation, the measurements of $n > 2$ Rényi entropies proposed here require full integer occupation detection. This requirement may be relaxed for hard-core interacting bosons, or specifically for *fermions*. An issue which we have not addressed here is the entanglement and negativity measurement protocols for fermions where additional fermionic exchange phases should be taken into account [38].

We have also attained field theory predictions for the distribution of entanglement in critical 1D systems and have verified them numerically. In addition to critical systems, one may study the symmetry decomposition of negativity in gapped systems. It would be interesting to further explore physical consequences of this imbalance decomposition of negativity in topological systems [21–23] such as the AKLT model [49,50].

ACKNOWLEDGMENTS

We thank Piet Brouwer for useful discussions. E.S. was supported in part by the Israel Science Foundation (Grant No. 1243/13) and by the US-Israel Binational Science Foundation (Grant No. 2016255). M.G. was supported by the Israel Science Foundation (Grant No. 227/15), the German Israeli Foundation (Grant No. I-1259-303.10), the US-Israel Binational Science Foundation (Grant No. 2016224), and the Israel Ministry of Science and Technology (Contract No. 3-12419).

APPENDIX A: GENERALIZED TQFT RESULTS

In this Appendix we investigate the fluxed twist operator $\mathcal{T}_n\mathcal{V}_\alpha$ of Sec. IV. Following Refs. [28,33,42], we find its scaling dimension (48) and show that it depends only on the total flux insertion. For simplicity, we set $K = 1$ (free fermions) within this appendix.

A vertex operator insertion of $\mathcal{V}_{\alpha_k}$ at copy $k = 1, \ldots, n$ creates a monodromy of α when crossing to the next copy. Therefore, the boson fields ϕ_k satisfy the relations upon crossing the A_1 cut at $[-\ell_1, 0]$,

$$\Psi \mapsto T_{\{\alpha\}}\Psi, \quad (A1)$$

where the field vector Ψ and transformation matrix $T_{\{\alpha\}}$ satisfy [51]

$$\Psi = \begin{pmatrix} e^{i\phi_1} \\ e^{i\phi_2} \\ \vdots \\ e^{i\phi_n} \end{pmatrix}, \quad T_{\{\alpha\}} = \begin{pmatrix} 0 & e^{i\alpha_1} & & \\ & 0 & e^{i\alpha_2} & \\ & & \ddots & \ddots \\ (-1)^{n+1}e^{i\alpha_n} & & & 0 \end{pmatrix}. \quad (A2)$$

This transformation matrix has eigenvalues

$$\lambda_p = e^{i\frac{1}{n}\sum_{k=1}^n \alpha_k} e^{2\pi i \frac{p}{n}}, \quad p = -\frac{n-1}{2} \cdots \frac{n-1}{2}. \quad (A3)$$

On the other hand, upon crossing the A_2 cut at $[0, \ell_2]$ the relation reverses

$$\Psi \mapsto T^{\mathrm{T}}_{\{-\alpha\}}\Psi. \quad (A4)$$

Since $T^{\mathrm{T}}_{\{-\alpha\}} = T^{\dagger}_{\{\alpha\}} = T^{-1}_{\{\alpha\}}$, one has $[T^{\mathrm{T}}_{\{-\alpha\}}, T_{\{\alpha\}}] = 0$. This enables one to simultaneously diagonalize the transformations $T_{\{\alpha\}}$ and $T^{\mathrm{T}}_{\{-\alpha\}}$ in the cuts A_1 and A_2. This implies that the p basis eigenvector fields ϕ_p remain decoupled and so all correlations depend only on $\alpha = \sum_{k=1}^n \alpha_k$. In agreement with the monodromies, one may decompose [33,42] the fluxed twist operator $(\mathcal{T}_n\mathcal{V}_\alpha) = \prod_p e^{i(\frac{p}{n} + \frac{\alpha}{2\pi n})\phi_p}$ and find its scaling dimension

$$\Delta_n(\alpha) = \frac{1}{2}\sum_p \left(\frac{p}{n} + \frac{\alpha}{2\pi n}\right)^2 = \frac{1}{24}\left(n - \frac{1}{n}\right) + \frac{1}{2n}\left(\frac{\alpha}{2\pi}\right)^2. \quad (A5)$$

Similar scaling dimensions may be found for the other fluxed twist operators.

APPENDIX B: NUMERICAL TECHNIQUE

In this Appendix we briefly review the double-Gaussian representation of Refs. [26,45] and use it to explicitly present our numerical procedure of Eq. (55), which is displayed in Fig. 4. References [26,45] have shown that the partially transposed density matrix of free-electron systems may be

written as a sum of Gaussian matrices

$$\rho_A^{T_2} = \sum_{\sigma=\pm} u_\sigma \frac{\hat{O}_\sigma}{\mathrm{Tr}\hat{O}_\sigma}, \tag{B1}$$

$$\hat{O}_\sigma = e^{\sum_{ij}\hat{c}_i^\dagger [W_\sigma]_{ij}\hat{c}_j}, \qquad u_\sigma = \frac{1}{\sqrt{2}} e^{-i(\pi/4)\sigma}. \tag{B2}$$

The W_σ matrices are related to the fermionic Green's function $[C]_{ij} = \langle[\hat{c}_i^\dagger, \hat{c}_j]\rangle$ by

$$e^{W_\sigma} = \frac{1+G_\sigma}{1-G_\sigma}, \quad G_\sigma = \left(\begin{array}{c|c} C^{11} & \sigma i C^{12} \\ \hline \sigma i C^{21} & C^{22} \end{array}\right), \tag{B3}$$

where $C^{\alpha\beta}$ are the blocks of C in regions A_α and A_β.

To obtain Eq. (55), we first study a generic quadratic operator $\hat{X} = \sum_{ij}\hat{c}_i^\dagger [X]_{ij}\hat{c}_j$,

$$\mathrm{Tr}\{e^{\hat{X}}(\rho_A^{T_2})^n\} = \sum_{\{\sigma\}} u_{\{\sigma\}} \frac{\mathrm{Tr}\{e^{\hat{X}}\prod_i \hat{O}_{\sigma_i}\}}{\prod_i \mathrm{Tr}\hat{O}_{\sigma_i}}, \tag{B4}$$

where $u_{\{\sigma\}} = 2^{-n/2} e^{-i(\pi/4)\sum_i \sigma_i}$ are the coefficients of $\{\hat{O}_\sigma\}$ in the expansion of $(\rho_A^{T_2})^n$. We use the results of Refs. [46,47] to evaluate

$$\mathrm{Tr}\{e^{\hat{X}}(\rho_A^{T_2})^n\} = \sum_{\{\sigma\}} u_{\{\sigma\}} \frac{\det\left(1 + e^X \prod_i e^{W_{\sigma_i}}\right)}{\prod_i \det(1+e^{W_{\sigma_i}})}. \tag{B5}$$

When $[X, W_\sigma] = 0$, we may use Eq. (B3) and some matrix algebra to get

$$\begin{aligned}\mathrm{Tr}\{e^{\hat{X}}(\rho_A^{T_2})^3\} = &-\frac{1}{2}\det\left[\left(\frac{1-G_+}{2}\right)^3 + e^X\left(\frac{1+G_+}{2}\right)^3\right] \\ &+ \frac{3}{2}\det\left[\left(\frac{1-G_+}{2}\right)^2\frac{1-G_-}{2}\right. \\ &\left. + e^X\left(\frac{1+G_+}{2}\right)^2\frac{1+G_-}{2}\right].\end{aligned} \tag{B6}$$

This may straightforwardly be numerically estimated.

As noted in Sec. IV, for the calculation of R_3 we pick $\hat{O} = i\alpha(\hat{N}_1 - \hat{N}_2^{T_2})$ in Eq. (55). However, in this basis [26] we have $\hat{N}_2^{T_2} = L_2 - \hat{N}_2$, where L_2 is the number of sites in A_2. Therefore, $\hat{O} = i\alpha(\hat{N} - L_2)$ and

$$[R_n]_Q = \int_{-\pi}^{\pi} \frac{d\alpha}{2\pi} e^{-i\alpha Q - i\alpha L_2}\mathrm{Tr}\{e^{i\alpha\hat{N}}(\rho_A^{T_2})^n\}, \tag{B7}$$

such that $\hat{N} = \sum_{ij}\hat{c}_i^\dagger[\mathbb{I}]_{ij}\hat{c}_j$ clearly satisfies $[\mathbb{I}, W_\sigma] = 0$, and we may use Eq. (B6).

[1] A. Peres, Phys. Rev. Lett. **77**, 1413 (1996).
[2] L. Amico, R. Fazio, A. Osterloh, and V. Vedral, Rev. Mod. Phys. **80**, 517 (2008).
[3] N. Laflorencie, Phys. Rep. **646**, 1 (2016).
[4] P. Ruggiero, V. Alba, and P. Calabrese, Phys. Rev. B **94**, 195121 (2016).
[5] K. Życzkowski, Phys. Rev. A **60**, 3496 (1999).
[6] J. Lee, M. Kim, Y. Park, and S. Lee, J. Mod. Opt. **47**, 2151 (2000).
[7] J. Eisert and M. B. Plenio, J. Mod. Opt. **46**, 145 (1999).
[8] G. Vidal and R. F. Werner, Phys. Rev. A **65**, 032314 (2002).
[9] M. B. Plenio, Phys. Rev. Lett. **95**, 090503 (2005).
[10] J. Eisert, Ph.D. thesis, University of Potsdam, 2001.
[11] J. Gray, L. Banchi, A. Bayat, and S. Bose, arXiv:1709.04923.
[12] P. Calabrese, J. Cardy, and E. Tonni, Phys. Rev. Lett. **109**, 130502 (2012).
[13] P. Calabrese, J. Cardy, and E. Tonni, J. Stat. Mech. (2013) P02008.
[14] P. Calabrese, J. Cardy, and E. Tonni, J. Phys. A: Math. Theor. **48**, 015006 (2014).
[15] M. Hoogeveen and B. Doyon, Nucl. Phys. B **898**, 78 (2015).
[16] A. Coser, E. Tonni, and P. Calabrese, J. Stat. Mech. (2016) 033116.
[17] C.-M. Chung, V. Alba, L. Bonnes, P. Chen, and A. M. Läuchli, Phys. Rev. B **90**, 064401 (2014).
[18] N. Yu, Phys. Rev. A **94**, 060101 (2016).
[19] R. Quesada, S. Rana, and A. Sanpera, Phys. Rev. A **95**, 042128 (2017).
[20] J. Tura, A. Aloy, R. Quesada, M. Lewenstein, and A. Sanpera, Quantum **2**, 45 (2018).
[21] Y. A. Lee and G. Vidal, Phys. Rev. A **88**, 042318 (2013).
[22] C. Castelnovo, Phys. Rev. A **88**, 042319 (2013).
[23] X. Wen, P.-Y. Chang, and S. Ryu, J. High Energy Phys. (2016) 12.
[24] P. Ruggiero, V. Alba, and P. Calabrese, Phys. Rev. B **94**, 035152 (2016).
[25] I. Burmistrov, K. Tikhonov, I. Gornyi, and A. Mirlin, Ann. Phys. (N.Y.) **383**, 140 (2017).
[26] V. Eisler and Z. Zimborás, New J. Phys. **17**, 053048 (2015).
[27] N. Laflorencie and S. Rachel, J. Stat. Mech. (2014) P11013.
[28] M. Goldstein and E. Sela, Phys. Rev. Lett. **120**, 200602 (2018).
[29] H. Barghathi, C. M. Herdman, and A. Del Maestro, arXiv:1804.01114.
[30] C. M. Alves and D. Jaksch, Phys. Rev. Lett. **93**, 110501 (2004).
[31] A. J. Daley, H. Pichler, J. Schachenmayer, and P. Zoller, Phys. Rev. Lett. **109**, 020505 (2012).
[32] R. Islam, R. Ma, P. M. Preiss, M. Eric Tai, A. Lukin, M. Rispoli, and M. Greiner, Nature (London) **528**, 77 (2015).
[33] A. Belin, L.-Y. Hung, A. Maloney, S. Matsuura, R. C. Myers, and T. Sierens, J. High Energy Phys. (2013) 59.
[34] A. Belin, L.-Y. Hung, A. Maloney, and S. Matsuura, J. High Energy Phys. (2015), 59.
[35] G. Pastras and D. Manolopoulos, J. High Energy Phys. (2014) 7.
[36] S. Matsuura, X. Wen, L.-Y. Hung, and S. Ryu, Phys. Rev. B **93**, 195113 (2016).

[37] H. Pichler, L. Bonnes, A. J. Daley, A. M. Läuchli, and P. Zoller, New J. Phys. **15**, 063003 (2013).
[38] E. Cornfeld, E. Sela, and M. Goldstein, arXiv:1808.04471.
[39] H. F. Song, S. Rachel, C. Flindt, I. Klich, N. Laflorencie, and K. Le Hur, Phys. Rev. B **85**, 035409 (2012).
[40] T. Giamarchi, *Quantum Physics in One Dimension* (Clarendon Press, Oxford, 2003).
[41] A. O. Gogolin, A. A. Nersesyan, and A. M. Tsvelik, *Bosonization and Strongly Correlated Systems* (Cambridge University Press, Cambridge, 2004).
[42] E. Cornfeld and E. Sela, Phys. Rev. B **96**, 075153 (2017).
[43] M. Fagotti and P. Calabrese, J. Stat. Mech. (2010) P04016.
[44] A. Coser, E. Tonni, and P. Calabrese, J. Stat. Mech. (2015) P08005.
[45] V. Eisler and Z. Zimborás, Phys. Rev. B **93**, 115148 (2016).
[46] I. Klich, arXiv:cond-mat/0209642.
[47] I. Klich, J. Stat. Mech. (2014) P11006.
[48] B.-Q. Jin and V. E. Korepin, J. Stat. Phys. **116**, 79 (2004).
[49] I. Affleck, T. Kennedy, E. H. Lieb, and H. Tasaki, Phys. Rev. Lett. **59**, 799 (1987).
[50] R. A. Santos, V. Korepin, and S. Bose, Phys. Rev. A **84**, 062307 (2011).
[51] H. Casini, C. D. Fosco, and M. Huerta, J. Stat. Mech. (2005) P07007.